



## Interlaminar fracture in woven carbon/epoxy laminates

Paulo N.B. Reis

*Department of Electromechanical Engineering, University of Beira Interior*  
*preis@ubi.pt*

José A.M. Ferreira, José D.M. Costa

*CEMUC, Department of Mechanical Engineering, University of Coimbra*  
*martins.ferreira@dem.uc.pt, jose.domingos@dem.uc.pt*

António M. Pereira

*ESTG/CDRsp, Polytechnic Institute of Leiria*  
*mario.pereira@ipleiria.pt*

---

**ABSTRACT.** This paper describes an experimental study developed to characterize the mode I and mode II fracture toughness of carbon/epoxy woven composites, using DCB and ENF tests, respectively. The laminates were manufactured using an epoxy resin and twelve woven balanced bi-directional layers of carbon fibres, all of them with the same orientation (0/90°). Significant instantaneous delaminations were observed particularly for the DCB specimen, which were responsible for an oscillatory behaviour of  $G_I$  versus crack length. The maximum values obtained for  $G_{IC}$  and  $G_{IIC}$  were 281 and 1800 J/m<sup>2</sup>, respectively.

**KEYWORDS.** Carbon fibre reinforced composites; Delamination; Fracture toughness; Mechanical testing.

---

### INTRODUCTION

Impacts at low velocity are the main cause of in-service delaminations, which are very dangerous because they are not easily detected visually [1, 2] and they can affect significantly the residual properties and structural integrity [3-8]. In this context, for design purpose it is very important to understand the interlaminar fracture toughness properties of fibre reinforced composite materials. If the double cantilever beam (DCB) test is one of the most popular to determine  $G_{IC}$ , because it presents simple specimen geometry and a stable crack growth in loading under displacement control, for mode II the most popular tests are the end-notched flexure (ENF), end-loaded split (ELS) and the four-point end-notched flexure (4ENF) [9]. However, according to the Morais and Pereira [9], the ENF specimen combined with the ECM (effective crack method) is the best solution for the characterization of mode II fracture with some advantages like simplicity, negligible friction effects and low tendency for geometric non-linearity.

For carbon fibre reinforced epoxies resins, it was found that the typical values of  $G_{IC}$  in stable propagation are around 260 J/m<sup>2</sup> [10]. In order to improve the interlaminar toughness of the composites materials the bibliography suggests the application of the thermoplastic resins [10], due their high damage tolerance, or by insertion of ductile resin interleaf between each carbon fibre/epoxy layers [11]. An alternative to the toughened resins is the use of advanced textile technologies with substantially improved delamination resistance [12, 13]. It was demonstrated that  $G_{IC}$  values for the knitted composites are about 10 or 20 times higher than for the uniweave composite [6]. Chen *et al.* [10] observed that the values of  $G_{IC}$ , in stable propagation, have a dropping tendency with increasing fibre content in the range 21-39% and

---

higher fibre bridging. The fibre direction was studied by Miyagawa *et al.* [14] and they found that the lowest values were obtained with samples whose fibre direction was 90°.

It is evident by the literature that the resistance to crack growth depends of the laminates, in terms of their constituents and set up. Therefore, the present paper describes an experimental study developed to characterize mode I and mode II fracture toughness using DCB and ENF tests, respectively, in carbon/epoxy woven composites.

## EXPERIMENTAL PROCEDURE

Composite laminate sheets were manufactured using twelve woven, balanced, bi-directional, layers of carbon fibres (with 196 g/m<sup>2</sup>) all of them with the same orientation 0/90°, and an epoxy resin matrix. Fibres and resin were hand placed in a mould. The mould was then put into a vacuum bag producing 0.1 MPa during 8 hours for curing at room temperature. The fibre volume fraction ( $V_f$ ) was 0.66 and the average plate thickness was 3 mm. Details about the manufacture process of the composites laminates can be found in previous work of the authors [15]. A 100 µm PTFE film was introduced into the plates during moulding of the laminates in order to generate the starter crack.

Fig. 1 shows the fibre distribution along the longitudinal direction. The fibre angle misalignment was determined using the Designer 6.0 software and an average angle of 5.2° was obtained, with a standard deviation of 1.7°.

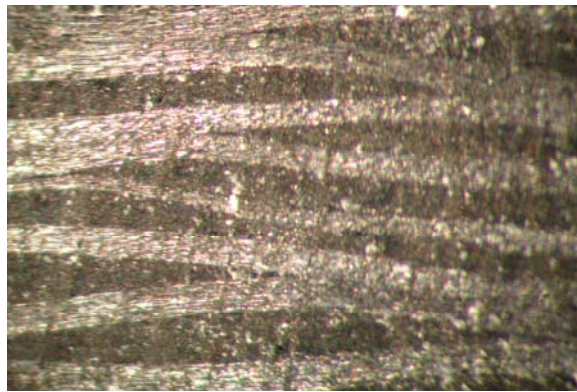


Figure 1: Lateral view photo showing the fibre distribution along of the longitudinal direction of the specimen.

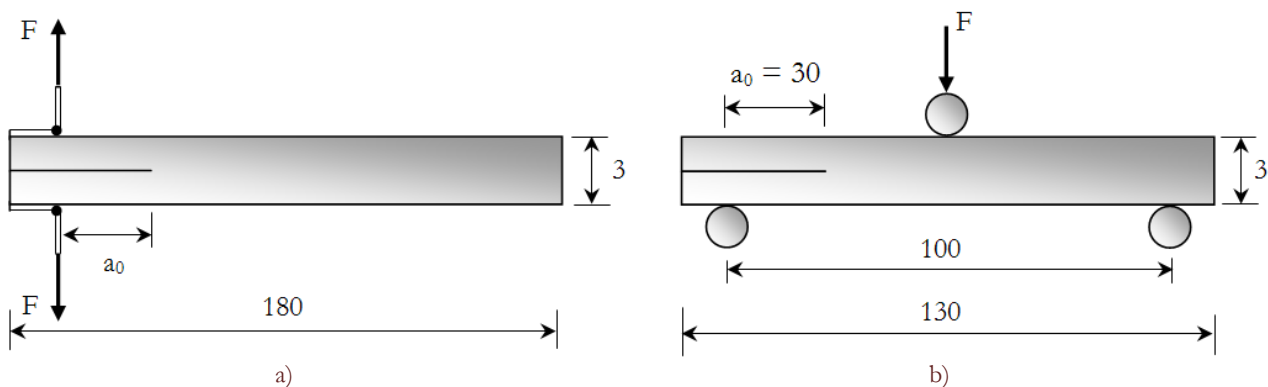


Figure 2: a) DCB specimen (Mode I); b) ENF specimen (mode II). Dimensions in mm.

The experimental work involved double cantilever beam (DCB) and end-notched flexure (ENF) tests. The specimens of composite material were cut by a diamond table saw from the original plates, 300 mm long and 100 mm wide, aligned with one fibre direction. The geometry and dimensions of the specimens are shown in Fig. 2. DCB specimens were used with 180 mm length, 25 mm width and initial crack lengths ( $a_0$ ) of 30, 45 and 50 mm. Two piano hinges were bonded to both surfaces of the specimen at the cracked end for load transmission. The piano hinges and the specimens were grit-blasted with sandpaper before bonding and cleaned with alcohol impregnated soft paper. The adhesive used for bonding was an Araldite 420 A/B bi-component. The DCB tests (Fig. 2a) were performed in tension, according to ASTM D 5528-

01 [16], using an electromechanical machine, Shimadzu model AG-X, equipped with a 1kN load cell. The ENF tests were carried out in the same machine in accordance with the literature [17, 18-19]. Fig. 2b is a schematic view of the three point bending apparatus and the specimens' dimensions with an initial crack ( $a_0$ ) of 30 mm. The load level, the displacement and the crack length were recorded during the tests. In order to obtain accurate results the crack length was measured using CCD camera, PCO model PixelFly 270 XS, as shown in Fig. 3.



Figure 3: DBC test apparatus with CCD camera video image.

For each condition four samples were tested and the experiments were carried out with the crosshead velocity of 0.5 mm/min for loading the samples [14]. In all samples one of the edges was painted with nail varnish and then several marks were made for determination of the crack length.

## RESULTS AND DISCUSSION

Fig. 4a and 4b show the experimental load-displacement curves from the DCB and ENF tests, respectively. Relatively to DCB tests, Fig. 4a, representative curves are presented for the initial cracks ( $a_0$ ) of 30, 45 and 50 mm. It is possible to observe that longer initial cracks produce curves with lower slopes. For the same displacement, the increase of initial crack length decreases the loads. All of them exhibit oscillatory behaviour, which is explained by the unstable crack propagation. In this case the load drops suddenly at a certain displacement and the crack propagates rapidly, increasing again the load with the displacement until a new drop occurs suddenly. According with several studies [11, 20-21] the unstable crack propagation is consequence of regions with different toughness. When the crack reaches the tougher region, it slows down until the rate of release of elastic stored energy is sufficient to propagate the crack through the tougher region. The release rate of stored energy is then higher than that required for stable growth. The crack then accelerates and unstable fracture occurs [20]. In fact it is possible to observe in Fig. 1 regions with reduced amounts of resin, where the fibres practically contact, while other regions are rich in resin. Therefore there are regions with different toughness which explain the unstable propagation observed. For mode II specimens (ENF), Fig. 4b presents two experimental load-displacement curves for  $a_0 = 30$  mm, which are reproducible and similar to other reported in literature [9, 14, 17]. An offset of 10 mm is represented between curves in order to obtain more details about their evolution. In this case unstable crack propagation was also observed but less significant.

Fig. 5 shows the interlaminar fracture toughness ( $G_I$ ) against the increment of the crack length ( $\Delta a$ ). Each value of  $G_I$  is an average of four tests. According to the ASTM D 5528-01 Standard [16], the MBT data reduction method was used because it promotes the most conservative values of  $G_{IC}$ . Therefore,  $G_{IC}$  was calculated by the following equation:

$$G_I = \frac{3.P.\delta}{2.b.(a + \Delta)} \quad (1)$$

where P is the load,  $\delta$  is the load contact point displacement, b is the specimen width, a is the delamination length and  $\Delta$  is the modulus of a correction factor. This factor is obtained experimentally by generating a least squares plot of the cube root of the compliance C against the delamination length a ( $\Delta$  is the value for  $C^{1/3}$  equal to zero).

It is possible to observe an initial stage, which is characterized by an increasing of the interlaminar fracture toughness ( $G_I$ ) with the crack length. After reaching a maximum value, or very close to it, is almost constant independently of crack length. This phenomenon agrees with Fig. 4, where the load increases with the increase of the displacement and, after a peak load, unstable crack propagation can be observed promoting an oscillatory behaviour of  $G_I$ .

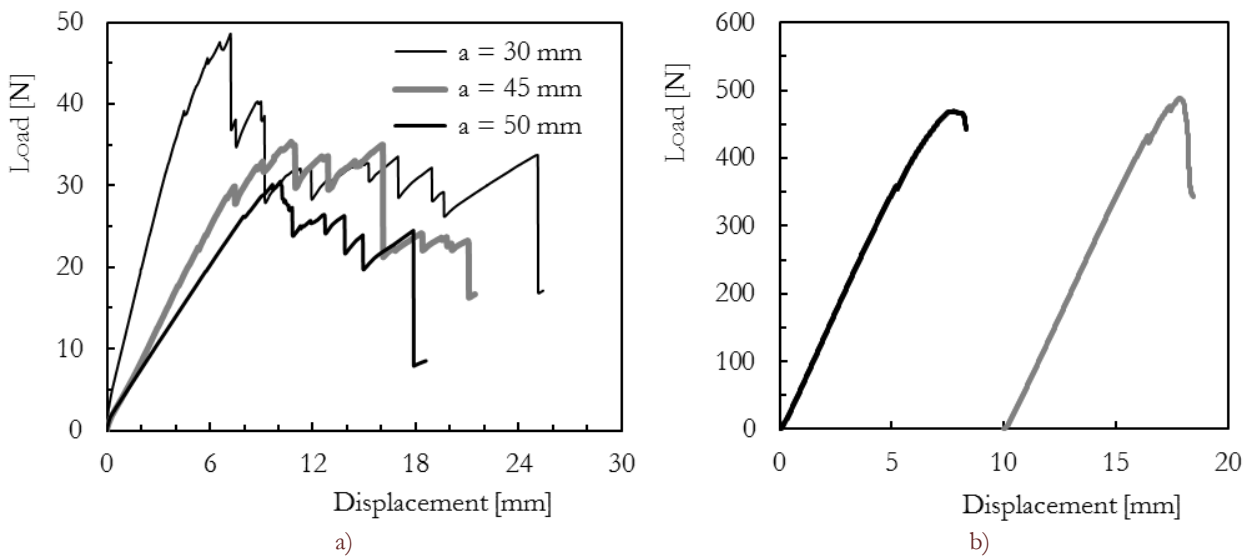


Figure 4: Typical load-displacement curves for: a) DCB tests, b) ENF tests.

$G_{IC}$  values for the different initial crack lengths are presented in Tab. 1. According to the ASTM D 5528-01 Standard [16], three definitions for an initiation value of  $G_{IC}$  can be used. In the present study the  $G_{IC}$  values were determined using the load and deflection measured at the point at which the compliance has increased by 5 % or the load has reached a maximum value (5 %/max) [16]. However, the intersection of the load-deflection curve occurs after the maximum load point for all tests performed. Therefore, the maximum load was used to calculate  $G_{IC}$  values according to the standard.

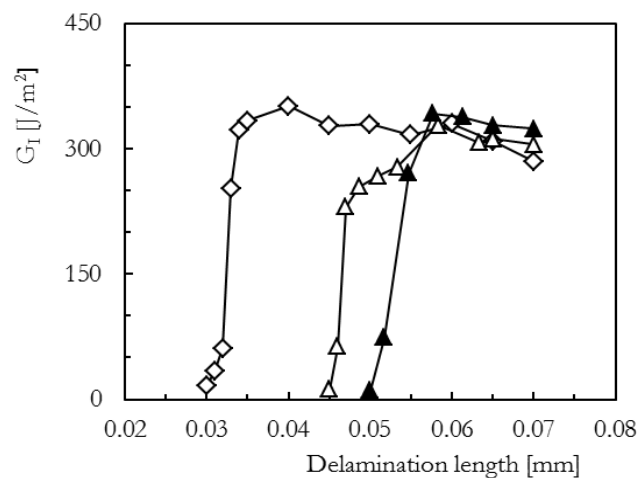


Figure 5:  $G_I$  versus crack length.



According with Tab. 1, it is possible to observe that only a small decrease of the interlaminar fracture toughness occurs, around 7.5%, which means that the  $G_{IC}$  parameter is practically independent of the initial delamination length. Therefore, for the present laminates, the average value of  $G_{IC}$  is around 281 J/m<sup>2</sup>.

	Initial crack length ( $a_0$ )		
	30 mm	45 mm	50 mm
$G_{IC}$ [J/m <sup>2</sup> ]	292.3	279.6	270.4
SD [J/m <sup>2</sup> ]	65.6	63.6	58.1

Table 1:  $G_{IC}$  values versus delamination length.

Fig. 6 presents the energy release rate for mode II specimens and the formulation used to obtain G can be found in the work of Morais and Pereira [9]. Therefore,  $G_{IIc}$  was calculated by the following equation:

$$G_{II} = \frac{9.P^2.a_e^2}{16.b^2.E_1.h^3} \quad (2)$$

where

P is the load,

b is the specimen width,

h is the specimen thickness,

$E_1$  is the flexural modulus

$a_e$  is expressed by the Eq. (3):

$$a_e = \sqrt[3]{\frac{8.E_1.b.h^3.C_f - 2.L^3}{3}} \quad (3)$$

where

L is half of the spam length (50 mm)

$C_f$  given by Eq. (4):

$$C_f = C - \frac{3.L}{10.\mu_{13}.b.h} \quad (4)$$

where

$\mu_{13}$  is the shear moduli

C the specimen compliance expressed by Eq. (5):

$$C \approx \frac{2.L^3 + 3.(a + \Delta_{II})^3}{8.E_1.b.h^3} + \frac{3.L}{10.\mu_{13}.b.h} \quad (5)$$

and, finally, for carbon fibers,  $\Delta_{II}$  is expressed by the following equation:

$$\Delta_{II} \approx h.\sqrt{\frac{E_1}{72.\mu_{13}}} \quad (6)$$



The  $G_{IIc}$  results obtained with the ENF specimen show a stable increase up to the peak value observed for an effective crack length of about 43 mm. The maximum values obtained for  $G_{IIc}$  is around 1800 J/m<sup>2</sup>.

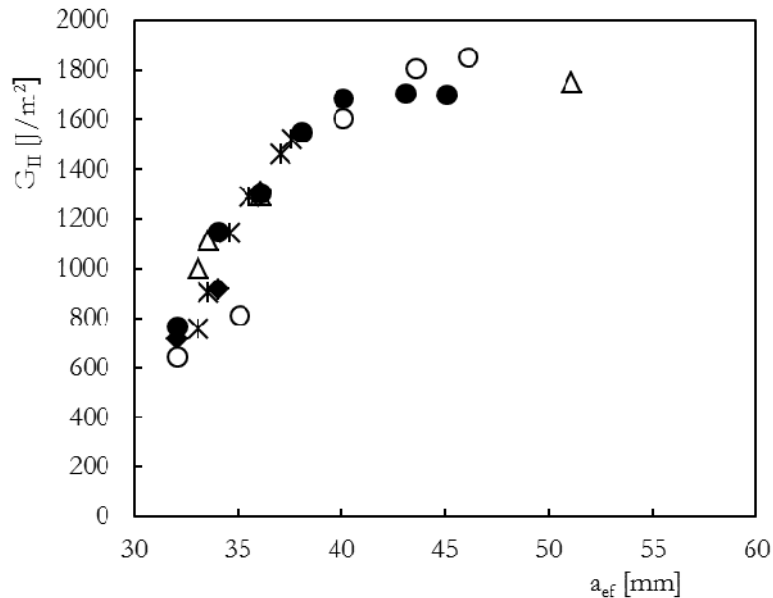


Figure 6:  $G_{II}$  versus crack length.

## CONCLUSIONS

The delamination of carbon-epoxy laminated composites was studied using mode I DCB specimen and mode II ENF specimens.

Notched specimens were prepared, and tested under quasi-static loading, in order to obtain the load-displacement curves and energy release rate versus crack length. Significant instantaneous delaminations were observed particularly for all the DCB specimen independently initial crack delamination length. The mode I critical energy release rate showed some oscillatory behaviour, explained by the instantaneous delaminations. The maximum values obtained for  $G_{IC}$  and  $G_{IIc}$  were 281 and 1800 J/m<sup>2</sup>, respectively.

## REFERENCES

- [1] Adams, R.D., Cawley, P.D., A Review of Defects Types and Non-Destructive Testing Techniques for Composites and Bonded Joints. *NDT Int.*, 21 (1998) 208-222.
- [2] Amaro, A.M., Reis, P.N.B., de Moura, M.F.S.F., Santos, J.B., Damage Detection on Laminated Composite Materials Using Several NDT Techniques. *Insight*, 54 (2012) 14-20.
- [3] Caprino, G., Residual Strength Prediction of Impacted CFRP Laminates. *J. Compos. Mater.*, 18 (1984) 508-518.
- [4] Davies, G.A.O., Hitchings, D., Zhou, G., Impact damage and residual strengths of woven fabric glass/polyester laminates. *Compos. Part A-Appl. S.*, 27 (1996) 1147-1156.
- [5] de Moura, M.F.S.F., Marques, A.T., Prediction of low velocity impact damage in carbon-epoxy laminates. *Compos. Part A-Appl. S.*, 33 (2002) 361-368.
- [6] Amaro, A.M., de Moura, M.F.S.F., Reis, P.N.B., Residual strength after low velocity impact in carbon-epoxy laminates. *Mater. Sci. Forum*, 514-516 (2006) 624-628.
- [7] Amaro, A.M., Reis, P.N.B., de Moura, M.F.S.F., Delamination effect on bending behaviour in carbon-epoxy composites. *Strain*, 47 (2011) 203-208.
- [8] Reis, P.N.B., Ferreira, J.A.M., Antunes, F.V., Richardson, M.O.W., Effect of Interlayer Delamination on Mechanical Behavior of Carbon/Epoxy Laminates. *J. Compos. Mater.*, 43 (2009) 2609- 2621.



- [9] Morais, A.B., Pereira, A.B., Application of the effective crack method to mode I and mode II interlaminar fracture of carbon/epoxy unidirectional laminates. *Compos. Part A-Appl. S.*, 38 (2007) 785-794.
- [10] Chen, J.H., Schulz, E., Bohse, J., Hinrichsen, G., Effect of fibre content on the interlaminar fracture toughness of unidirectional glass-fibre/polyamide composite. *Compos. Part A-Appl. S.*, 30 (1999) 747-755.
- [11] Matsuda, S., Hojo, M., Ochiai, S., Murakami, A., Akimoto, H., Ando, M., Effect of ionomer thickness on mode I interlaminar fracture toughness for ionomer toughened CFRP. *Compos. Part A-Appl. S.*, 30 (1999) 1311-1319.
- [12] Kim, K.Y., Curiskis, J.I., Ye, L., Fu, S.Y., Mode I interlaminar fracture behaviour of weft-knitted fabric reinforced composites. *Compos. Part A-Appl. S.*, 36 (2005) 954-964.
- [13] Mouritz, A.P., Bains, C., Herszberg, I., Mode I interlaminar fracture toughness properties of advanced textile fiberglass composites. *Compos. Part A-Appl. S.*, 30 (1999) 859-870.
- [14] Miyagawa, H., Sato, C., Ikegami, K., Interlaminar fracture toughness of CFRP in mode I and mode II determined by Raman spectroscopy. *Compos. Part A-Appl. S.*, 32 (2001) 477-486.
- [15] Reis, P.N.B., Ferreira, J.A.M., Costa, J.D.M., Richardson, M.O.W., Fatigue life evaluation for carbon/epoxy laminate composites under constant and variable block loading. *Compos. Sci. Technol.*, 69 (2009) 154-160.
- [16] Standard test method for Mode I interlaminar fracture toughness of unidirectional fiber-reinforced polymer matrix composites, ASTM Standard D 5528-01. Philadelphia, PA: American Society for Testing and Materials, 2001.
- [17] Pereira, A.B., Morais, A.B., Mode II interlaminar fracture of glass/epoxy multidirectional laminates. *Compos. Part A-Appl. S.*, 35 (2004) 265-272.
- [18] Davies, P., Blackman, B.R.K., Brunner, A.J., Standard test methods for delamination resistance of composite materials: current status. *Appl. Compos. Mater.*, 5 (1998) 345-364.
- [19] Davies, P., Sims, G.D., Blackman, B.R.K., Brunner, A.J., Kageyama, K., Hojo, M., Tanaka, K., Murri, G., Rousseau, C., Gieseke, B., Martin, R.H., Comparison of test configurations for determination of mode II interlaminar fracture toughness: results from international collaborative test programme. *Plast. Rubber Compos.*, 28 (1999) 432-437.
- [20] Kotaki, M., Hamada, H., Effect of interfacial properties and weave structure on mode I interlaminar fracture behaviour of glass satin woven fabric composites. *Compos. Part A-Appl. S.*, 28 (1997) 257-266.
- [21] Ozdil, F., Carlsson, L.A., Mode I interlaminar fracture of interleaved graphite/epoxy. *J. Comp. Mater.*, 26 (1992) 433-458.